

Ion Channels

Cation-Transporting Peptides: Scaffolds for Functionalized Pores?

Harekrushna Behera, Venkatachalam Ramkumar, and Nandita Madhavan^{*[a]}

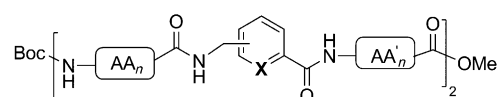
Abstract: Protein pores that selectively transport ions across membranes are among nature's most efficient machines. The selectivity of these pores can be exploited for ion sensing and water purification. Since it is difficult to reconstitute membrane proteins in their active form for practical applications it is desirable to develop robust synthetic compounds that selectively transport ions across cell membranes. One can envision tuning the selectivity of pores by incorporating

functional groups inside the pore. Readily accessible octapeptides containing (aminomethyl)benzoic acid and alanine are reported here that preferentially transport cations over halides across the lipid bilayer. Ion transport is hypothesized through pores formed by stable assemblies of the peptides. The aromatic ring(s) appear to be proximal to the pore and could be potentially utilized for functionalizing the pore interior.

Introduction

Pore-forming proteins that selectively transport ions across membranes play a vital role in cellular processes.^[1] A selectivity filter inside these pores has been shown to dictate its ion preference.^[1,2] Robust synthetic ion channels have been developed that mimic the activity of natural proteins.^[3] Synthetic pore-forming compounds have found application as antibacterial drugs, molecular switches, catalysts, and sensors.^[4] Placement of functional groups inside the pore is highly desirable for the aforementioned applications. The pore α -Hemolysin has been used for stochastic sensing of small molecules, charged species, and DNA.^[5] The selectivity of the Hemolysin pore for analytes has been tuned by placement of functional groups inside the pore through genetic engineering or incorporation of macrocyclic adapters inside the pore.

There are few examples of synthetic peptide-based internally functionalized pores. Cyclic peptides containing a repeating LLLD^[6] or an LD amino acid sequence with aromatic^[7] or tetrahydrofuran^[8] units have been shown to give functionalized pores. Pores obtained through the assembly of peptides appended to octaphenyl rods also place functional groups in the pore.^[3b,9] Herein, we report octapeptides **1–3**, containing (aminomethyl)benzoic acid groups (Figure 1). We had previously incorporated aminobenzoic acid units into the peptide scaffold.^[10] In peptides **1–3**, an sp^3 center is incorporated in addition to the turn-inducing aminobenzoic acid unit to provide conformational flexibility to the peptides. The sequence in peptides **2** and **3** is found to be most active for transporting



1a: *m*-, **X** = CH; **1b:** *p*-, **X** = CH; **AA_n** = DAlaLAla, **AA'_n** = LAla
2a: *m*-, **X** = CH; **2b:** *p*-, **X** = CH; **3:** *m*-, **X** = N; **AA_n** = LAla, **AA'_n** = LAlaDAla

Figure 1. Proposed scaffolds for functionalized pores.

ions across the lipid bilayer. The most active peptide **3** transports cations and not halides across the lipid bilayer. The peptides form stable assemblies and appear to form pores with the aromatic rings proximal to the pore. These aromatic rings could be potentially useful sites for internally functionalizing the pore.

Results and Discussion

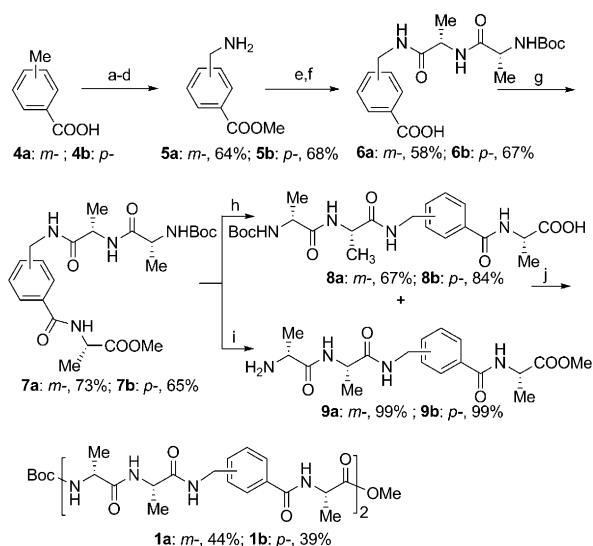
Octapeptides **1a** and **1b**, containing *m*- and *p*-substituted aromatic units, were synthesized in solution as shown in Scheme 1.^[11] The (methylamino)benzoic acid derivative **5** was synthesized, starting from the corresponding toluic acid isomer **4** in four steps. Sequential coupling and deprotection steps were subsequently carried out to afford peptides **1a** and **b**.

Transmission electron microscopy (TEM) images obtained after incubating the peptides in solution for 12 h, indicated that peptides **1a** and **b** aggregate to form bundles of nanofibers (Figure 2). The bundles with peptide **1b** were found to be slightly wider (28–38 nm) than those with peptide **1a** (15–30 nm).

The peptide **1a** was also found to form a stable three-dimensional assembly in the solid state. The crystal packing of peptide **1a** showed a pore (4–5 Å wide) lined with carbonyl groups that held water molecules inside by hydrogen-bonding (Figure 3a).^[12] Four intramolecular hydrogen bonds stabilize the folded structure of the peptide, while one intermolecular bond stabilizes the assembly (Figure 3b). We found it interesting that peptide **1a** crystallized with trace amounts of water

[a] H. Behera, V. Ramkumar, Dr. N. Madhavan
Department of Chemistry
Indian Institute of Technology, Madras
Chennai - 600036, Tamil Nadu (India)
E-mail: nanditam@iitm.ac.in

Supporting information for this article is available on the WWW under <http://dx.doi.org/10.1002/chem.201500881>.



Scheme 1. General procedure for synthesis of peptide **1**. a) SOCl_2 , MeOH, 0°C to RT, 5 h; b) NBS, AIBN, CH_2CN , 70°C , 16 h; c) NaN_3 , DMF, 80°C , 14 h; d) PPh_3 , THF, H_2O , 18 h; e) BocNHdAlaLAlaOH , HCTU, DIEA, CH_2Cl_2 , 0°C to RT, 12 h; f) LiOH, MeOH, H_2O , 4 h; g) L-Ala-OMe, HCTU, DIEA, THF, DMF, 0°C to RT, 15 h; h) LiOH, MeOH, H_2O , 3 h; i) TFA, CH_2Cl_2 , 0°C to RT, 4 h; j) HCTU, DIEA, DMF, 0°C to RT, 15 h (AIBN = azobisisobutyronitrile, Boc = *tert*-butoxycarbonyl, Ala = alanine, HCTU = O-(6-chlorobenzotriazol-1-yl)-*N,N,N',N'*-tetramethyluronium hexafluorophosphate, DIEA = *N,N*-diisopropylethylamine, TFA = trifluoroacetic acid).

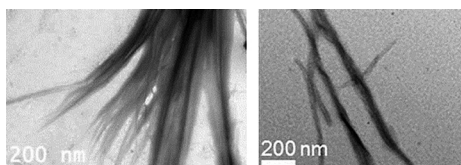


Figure 2. TEM images of peptides (0.5 mg mL^{-1}); left) **1a**; right) **1b**.

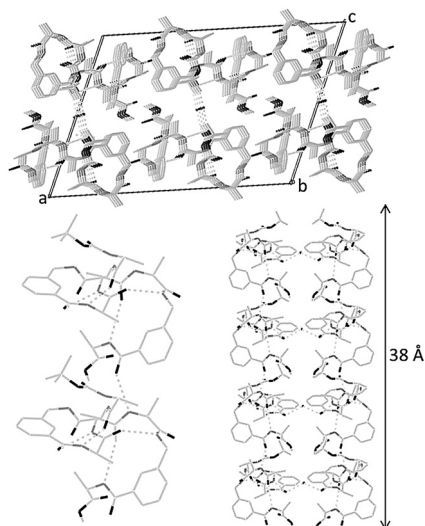


Figure 3. Top) Crystal packing for peptide **1a** indicating water-filled pores. Bottom left) Magnified image of peptide dimer illustrating the stabilizing interactions. Bottom right) Model for pore formation by peptide **1a**. Hydrogens omitted for clarity. Oxygens shown in black.

present in methanol to give such assemblies containing water-filled pores. If the peptide structure in the lipid bilayer is similar to its crystal structure, at least eight peptide units would be required to span the approximately 40 \AA thick membrane (Figure 3c). While the crystal structure cannot be directly correlated to the peptide structure in the bilayer, a viable conclusion from the microscopy as well as the crystal structure is that the peptides have a tendency to self-assemble to form tubelike structures.

Ion transport through the peptides was assessed using vesicles entrapped with pH-sensitive 8-hydroxypyrene-1,3,6-trisulfonic acid trisodium salt (HPTS) dye at pH 7.2.^[13] Based on the microscopy studies, peptide solutions were allowed to stand in solution (to ensure self-assembly) for at least 12 h before the experiment was conducted. The vesicles were incubated with peptides for 1–2 min, following which 0.5 N NaOH was added to introduce a pH gradient of 0.6 units (Figure 4a). The fluores-

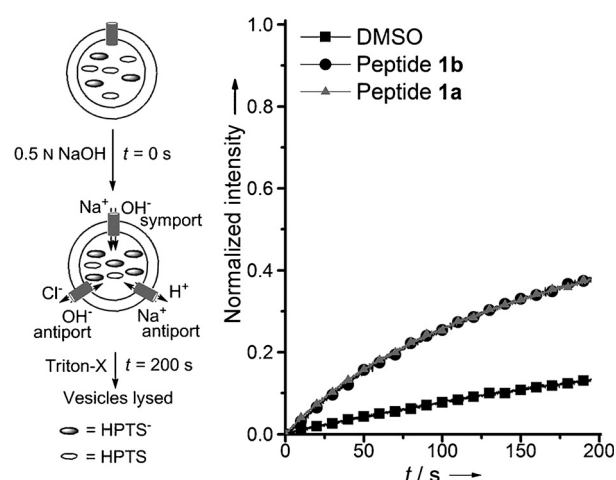


Figure 4. The HPTS assay for ion transport. Left) Schematic representation (channel mechanism). Right) Comparison of rate of change of HPTS^- concentration in the presence of peptides **1** ($100\text{ }\mu\text{M}$, $27\text{ mol}\%$) and DMSO.

cence intensity of deprotonated HPTS (HPTS^-) was monitored after addition of NaOH to determine transport activity of the peptides. A gradual increase in HPTS^- concentration was observed in the presence of peptides **1a** and **b**. (Figure 4b). Because the experiment is carried out with a concentration gradient of Na^+ and OH^- , this pH increase might be attributed to Na^+ entry into the vesicles, coupled with OH^- entry (symport), or H^+ exit (antiport) from the vesicles. An OH^-/Cl^- antiport mechanism could also be operative. At the end of the experiment a detergent Triton X was added to lyse the vesicles and the final intensity obtained was used to normalise the HPTS^- intensities (Figure 4b). The assay indicated that peptides **1a** and **b** were not that active. Dynamic light scattering (DLS) studies were carried out to ascertain that peptides **1a** and **1b** did not lyse the vesicles similar to Triton X.^[11]

Because peptides **1** were not very active, peptides **2a** and **2b** that contain the sequence of our previously reported aminobenzoic incorporated peptides were synthesized. Peptide **3**, which is the pyridyl analog of peptide **2a** was also synthesized.^[11] TEM and SEM were used to compare the aggregation

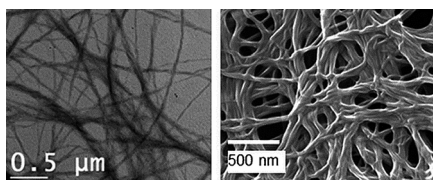


Figure 5. Left) TEM image of peptide 2a. Right) SEM image of peptide 3.

of peptides 2a and 3 (Figure 5). Bundles of nanofibers were seen in both cases. Interestingly a twisting of the fibers to give helical-type assemblies was observed for peptide 3 (Figure 5b).^[11]

The HPTS assay was carried out with peptides 2 and 3 and the ion-transport rates were obtained by fitting the curves to a first-order exponential equation. As seen from Table 1, peptide 2a was 1.4 times more active than 1a and peptide 2b, containing the *p*-substituted aromatic unit, was twice as active as peptide 1b. Peptide 3 was found to be more active than its benzyl analog (entry 5).

Entry	Peptide	k [$\times 10^{-3} \text{ s}^{-1}$] ^[c]
1	1a ^[a]	11.5 ± 2.0
2	1b ^[a]	11.3 ± 2.1
3	2a ^[a]	15.6 ± 2.5
4	2b ^[a]	23.2 ± 4.7
5	3 ^[b]	22.0 ± 1.2

[a] 100 μM, 27 mol%. [b] 50 μM, 13.5 mol%. [c] Avg. value. Individual k values calculated by fitting the curve using Origin 8.5.

To determine the anion selectivity of the most active peptide 3, vesicles entrapped with halide sensitive lucigenin dye were prepared.^[14] The fluorescence of lucigenin dye is reported to quench in the presence of halides. Aqueous solutions of sodium chloride or bromide (2N) were added to the vesicles, following which peptide solution was added (Figure 6a). The fluorescence intensity of the dye was normalized based on the final intensity obtained with Triton X. Quenching of lucigenin fluorescence upon adding peptide 3 was found to be similar to background transport (Figure 6b and c) indicating that peptide-mediated halide transport was minimal.

The lucigenin assay rules out an OH⁻/Cl⁻ antiport mechanism in the HPTS assay indicating that M⁺ transport might be dominant (Figure 4a). To confirm cation transport, a ²³Na NMR assay was carried out with peptide 3 (Figure 7a).^[15] A shift reagent was added to large vesicles (prepared in aqueous NaCl) so that distinct peaks could be seen for the internal and external Na⁺ ions. A broadening of the Na⁺ peaks was observed upon adding peptide, which indicated Na⁺ exchange (Figure 7b). The rate constant for Na⁺ exchange was determined using Equation (1), where ν_p and ν_0 correspond to the line width of the internal Na⁺ peak in the presence and absence of peptide, respectively.

$$k = \pi(\nu_p - \nu_0) \quad (1)$$

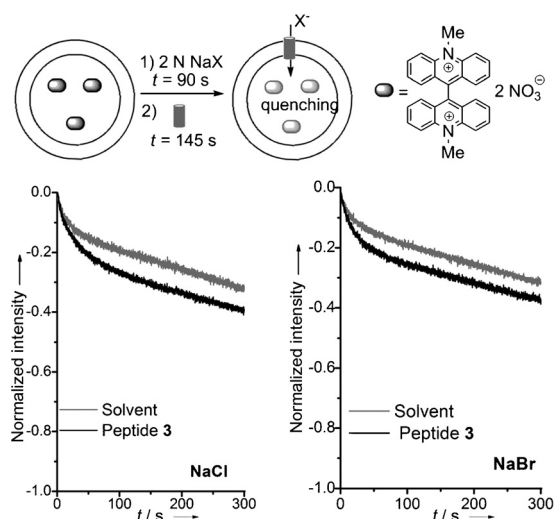


Figure 6. Lucigenin assay for halide transport: Top) Schematic representation. b) Fluorescence versus time plots with peptide 3 (50 μM, 13.5 mol%) in the presence of bottom left) NaCl, bottom right) NaBr. The time at which peptide was added has been considered as the beginning of the experiment (i.e., $t = 0$ sec in the x axis).

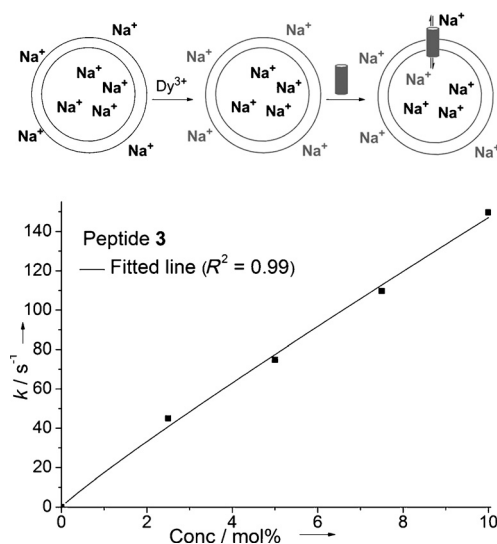


Figure 7. The ²³Na NMR assay. Top) Schematic representation. Bottom) k versus concentration plot.

The k values were found to be directly proportional to the concentration of peptide 3 (Figure 7b). In the assay, the peptides were added after an incubation period of at least 12 h in solution, to ensure peptide self-assembly. The microscopy studies show that the peptides assemble in this time period and the crystal structure also shows water-filled pores. Therefore, the linear correlation between the rate constant and the peptide concentration can be explained by the formation of a pore by a thermodynamically stable self-assembly of the peptides.^[16] A monomolecular pore is ruled out because it would be difficult for a single peptide to efficiently span the lipid bilayer. A carrier mechanism is also unlikely as it would not be very feasible for a peptide assembly to ferry back and forth the lipid bilayer as a carrier.

The HPTS, ^{23}Na NMR, and lucigenin experiments show that our peptides prefer to transport cations over halides. To see how the ion-transport activity varied with the concentration of peptides in the HPTS assay (Figure 4a), the experiment was carried out with varying concentrations of peptide **3** (Figure 8a).^[16a,c] The graph of fluorescence intensity (*I*) just before

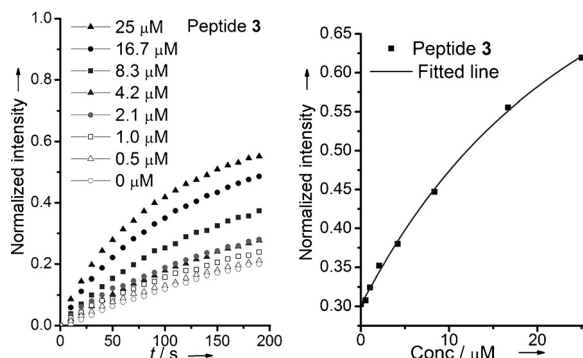


Figure 8. Hill analysis of peptide **3** Left) Fluorescence versus time plot with variable concentrations of peptide **3**. Right) Hill plot for peptide **3**.

addition of Triton X versus peptide concentration (*c*) was fitted to Equation (2), that is, the Hill equation (Figure 8b, Table 2).

$$I = I_{\infty} + ((I_0 - I_{\infty}) / (1 + (c/EC_{50})^n)) \quad (2)$$

In Equation (2), the intensities " I_{∞} " and " I_0 " correspond to the normalized fluorescence intensity with excess of peptide and no peptide, respectively. The EC_{50} value corresponds to the peptide concentration required to obtain half of the maximum fluorescence intensity and " n " corresponds to the Hill coefficient or the number of peptides that come together to interact with a single ion. The Hill coefficient was found to be close to 1 for peptide **3** (Table 2), corroborating the conclusion from the NMR experiment that the pore was formed by a stable peptide assembly.^[16] The Hill analysis was carried out with peptides **2a** and **2b** as well and, in all cases, the Hill coefficient was found to be close to 1 (Table 2).

The EC_{50} values obtained from the Hill analyses of peptides **2a**, **2b**, and **3** (Table 2), show that peptide **2b** is 1.4 times more active than **2a**, whereas peptide **3** is most active, that is, 1.8 times more active than its benzyl analog **2a**. The pyridyl ring could, in principle, act as a base and deprotonate the HPTS dye. Control experiments with the HPTS dye and pep-

Table 2. Comparison of EC_{50} and n values for peptides 2 and 3			
Entry	Peptide	EC_{50} [μM] ^[a,b]	n ^[b]
1	2a	51	1.3
2	2b	36	1.41
3	3	28	1.04

[a] 50 μM , 13.5 mol%. [b] Hill coefficient, obtained by fitting the Hill plots to Equation (2) using Origin 8.5.

ptides **2a** and **3** indicated no difference in the emission intensity of HPTS⁻ in the presence of **2a** and **3** (Figure S12 and S13 in the Supporting Information). The main difference between peptides **2a** and **3** is the presence of nitrogen atoms at the 2-positions of the aromatic rings. Because these pores prefer to transport cations over halides, the higher activity of peptide **3** alludes to the proximity of at least one of these electron-rich nitrogens (i.e., aromatic rings) to the pore interior. Hence, the aromatic ring(s) in peptide **2a** can potentially be used for the easy introduction of functional groups inside the pore.

Conclusion

In conclusion, acyclic octapeptides **1** containing (aminomethyl)benzoic acid units and alanine were developed and found to self-assemble to form nanotubes stabilized by hydrogen-bonding interactions. Ion-transport studies indicated that they were not very active. Therefore second generation peptides **2** and **3** were synthesized. Peptides **2** and **3** were found to self-assemble to form nanotubes and ion-transport studies showed that they were more active than the first-generation peptides. The HPTS, ^{23}Na NMR, and lucigenin assays indicated that the most active peptide **3** prefers to transport cations over halides. ^{23}Na NMR/HPTS assays with variable concentrations of peptide and microscopy studies indicate that these peptides form pores through highly stable assemblies. Hill analysis also indicated that peptide **3** ($EC_{50} = 28 \mu\text{M}$) was the most active peptide and was more active than its benzyl analog, that is, peptide **2a** ($EC_{50} = 51 \mu\text{M}$). The higher activity of peptide **3** is attributed to an increased pore electron density due to the presence of nitrogen atom(s) close to the pore. If indeed even a single aromatic ring is proximal to the pore, one can envision using it to functionalize the pore. Current efforts are focused on determining the nature of the ion-transporting pore and improving the activity of these pores through functionalization of the aromatic units.

Experimental Section

Ion transport studies with peptides using the HPTS assay

Preparation of vesicles:^[17,13c] To a solution of EYPC lipids (28.4 mg, 36.9 μmol , 9 equiv) in chloroform (0.284 mL), cholesterol (1.6 mg, 4.1 μmol , 1 equiv) was added and the solution was incubated for 5 min at 0 °C. Chloroform was removed by applying a stream of nitrogen gas. The resultant thin film was kept in vacuo for 5 h at 0 °C, following which 1 mL of HEPES buffer at pH 7.2 with HPTS dye (0.1 mM HPTS, 100 mM NaCl, 10 mM HEPES) was added. The resulting suspension was allowed to stir for 1 h at RT and then subjected to eight freeze-thaw (liq. N_2 and 40 °C) cycles. The vesicle mixture was sonicated in a bath sonicator at 0–5 °C for a total time of 2 min (30 s on and 30 s off in degass mode). The mixture was extruded 40 times through 100 nm polycarbonate membrane using a mini-extruder.^[18] The extra-vesicular dye was removed by size-exclusion chromatography using Sephadex G-50 (eluent: HEPES buffer at pH 7.2, 100 mM NaCl, 10 mM HEPES). The vesicle solution was collected and the total volume was made up to 2.5 mL with HEPES buffer at pH 7.2.

The HPTS assay:^[13c] Vesicle solution (75 μL) and HEPES buffer (2.9 mL) were placed in a cuvette. An appropriate amount of linear octapeptide in DMSO (10 μL) was added to the cuvette and the solution was allowed to stir for 30 s prior to the fluorescence experiment. After 50 s from the start of the experiment, NaOH (20 μL , 0.5 N) was added and at 250 s aqueous Triton X (TX; 5%, 50 μL) was added.

Lucigenin assay for halide transport

Preparation of vesicles: To a solution of dehydrogenated EYPC (18.8 mg) in chloroform was added cholesterol (1.2 mg). The lipid solution was incubated for 5 min at 0 °C. Chloroform was removed under a stream of nitrogen gas. The resultant thin film was kept in vacuo for 4 h at 0 °C and rehydrated with 1 mL of lucigenin dye (1.0 mM dye in 225 mM NaNO₃ solution). The suspension was swirled for 5–10 min and subsequently sonicated at 0 °C in a bath sonicator for 2 min (30 s on and 30 s off in degass mode). The vesicle solution was subjected to eight freeze-thaw cycles (liq N₂ and 40 °C) and extruded ten times through a 0.1 μm polycarbonate membrane. The extravesicular dye was removed by size exclusion chromatography using a G-50 sephadex column. The total collected volume was 2.0 mL.

Lucigenin assay with peptide 3: Vesicle solution (100 μL) and 2.9 mL of 225 mM NaNO₃ buffer were placed in a cuvette. At 91 s, 36 μL of 2 N NaX (X = Cl⁻, Br⁻) and at 145 s an appropriate amount of linear octapeptide 3 in 2.5% DMSO/MeOH (10 μL) was added to the vesicle solution. Finally, at 450 s, aqueous Triton X (5%, 50 μL) was added to the cuvette.

Ion transport study with peptide 3 using sodium NMR

Preparation of vesicles:^[13c,17a] To a solution of EYPC lipids (28.4 mg, 36.9 μmol , 9 equiv) in chloroform (0.284 mL), cholesterol (1.6 mg, 4.1 μmol , 1 equiv) was added and the solution was incubated for 5 min at 0 °C. Chloroform was removed by applying a stream of argon gas. The resultant thin film was kept in vacuo for 5 h at 0 °C, following which it was rehydrated with 1 mL of 200 mM NaCl. The resulting suspension was allowed to stir for 45 min at RT and then subjected to eight freeze-thaw (liq. N₂ and 40 °C) cycles. The vesicle mixture was sonicated in a bath sonicator at 0–5 °C for a total time of 2 min (30 s on and 30 s off in degass mode). The mixture was extruded 15 times through a 400 nm membrane to give the large unilamellar vesicle (LUV) solution.^[18] The vesicle solution and sample prepared for NMR study were stored in 1.5 mL Eppendorf vials.

Preparation of shift reagent: The shift reagent was prepared by mixing aqueous DyCl₃ (1 mL, 0.1 M) with aqueous sodium-tris(polyphosphate) solution (2 mL, 0.2 M).

NMR experiment: The LUV Vesicle solution (180 μL) was placed in a vial, following which D₂O (100 μL) and shift reagent (100 μL) were added. The solution was incubated at room temperature for 40 min. An appropriate amount of octapeptide 3 in DMSO (10 μL) was added to the vial and the solution was transferred to the NMR tubes. For the control experiment, the same procedure was used except DMSO (10 μL) was added instead of peptide 3.

Additional Information

Crystal structure information: CCDC-1008786 (1a) contains the supplementary crystallographic data for this paper. These data can be obtained free of charge from The Cambridge Crystallographic Data Centre via www.ccdc.cam.ac.uk/data_request/cif.

Supplementary information: detailed procedures, characterization of compounds, raw plots for assays, DLS data, and CD data has been provided in the Supporting Information.

Acknowledgements

This research was supported by DST (SR/S1/OC-41/2009), New Delhi, India. H.B. thanks IIT Madras for fellowship. We thank Dr. E. Prasad for the use of his DLS instrument and J. Mahita for her contribution towards synthesis of peptide 1b. We thank Mr. Karthikeyan for help with the ²³Na NMR experiments.

Keywords: cation transport • ion transport • nanotube • peptides • pores

- [1] B. Hille, *Ion Channels of Excitable Membranes*, 3rd ed., Sinauer, Sunderland, MA, 2001.
- [2] D. A. Doyle, J. M. Cabral, R. A. Pfuetzner, A. Kuo, J. M. Gulbis, S. L. Cohen, B. T. Chait, R. MacKinnon, *Science* **1998**, *280*, 69–77.
- [3] a) P. Reiß, U. Koert, *Acc. Chem. Res.* **2013**, *46*, 2773–2780; b) F. De Riccardis, I. Izzo, D. Montesarchio, P. Tecilla, *Acc. Chem. Res.* **2013**, *46*, 2781–2790; c) A. Vargas Jentzsch, A. Hennig, J. Mareda, S. Matile, *Acc. Chem. Res.* **2013**, *46*, 2791–2800; d) G. W. Gokel, S. Negin, *Acc. Chem. Res.* **2013**, *46*, 2824–2833; e) T. M. Fyles, *Acc. Chem. Res.* **2013**, *46*, 2847–2855; f) J. K. W. Chui, T. M. Fyles, *Chem. Soc. Rev.* **2012**, *41*, 148–175; g) S. Matile, A. V. Jentzsch, J. Montenegro, A. Fin, *Chem. Soc. Rev.* **2011**, *40*, 2453–2474; h) N. Sakai, J. Mareda, S. Matile, *Mol. Biosyst.* **2007**, *3*, 658–666; i) G. W. Gokel, I. A. Carasel, *Chem. Soc. Rev.* **2007**, *36*, 378–389; j) U. Koert, J. R. Pfeifer, *Synthesis* **2004**, *2004*, 1129–1146.
- [4] a) F. Xia, W. Guo, Y. Mao, X. Hou, J. Xue, H. Xia, L. Wang, Y. Song, H. Ji, Q. Ouyang, Y. Wang, L. Jiang, *J. Am. Chem. Soc.* **2008**, *130*, 8345–8350; b) E. C. Yusko, J. M. Johnson, S. Majd, P. Prangkiro, R. C. Rollings, J. Li, J. Yang, M. Mayer, *Nat. Nanotechnol.* **2011**, *6*, 253–260; c) V. Dartois, J. Sanchez-Quesada, E. Cabezas, E. Chi, C. Dubbelde, C. Dunn, J. Granja, C. Gritzen, D. Weinberger, M. R. Ghadiri, *Antimicrob. Agents Chemother.* **2005**, *49*, 3302–3310; d) R. S. Hector, M. S. Gin, *Supramol. Chem.* **2005**, *17*, 129–134; e) Q. H. Nguyen, M. Ali, R. Neumann, W. Ensinger, *Sens. Actuators B* **2012**, *162*, 216–222; f) N. Sorde, G. Das, S. Matile, *Proc. Natl. Acad. Sci. USA* **2003**, *100*, 11964–11969.
- [5] a) H. Bayley, P. S. Cremer, *Nature* **2001**, *413*, 226–230; b) J. Clarke, H.-C. Wu, L. Jayasinghe, A. Patel, S. Reid, H. Bayley, *Nat. Nanotechnol.* **2009**, *4*, 265–270; c) N. Ashkenasy, J. Sanchez-Quesada, H. Bayley, M. R. Ghadiri, *Angew. Chem. Int. Ed.* **2005**, *44*, 1401–1404; *Angew. Chem.* **2005**, *117*, 1425–1428.
- [6] D. Wang, L. Guo, J. Zhang, L. R. Jones, Z. Chen, C. Pritchard, R. W. Roeske, *J. Pept. Res.* **2001**, *57*, 301–306.
- [7] R. Hourani, C. Zhang, R. van der Weegen, L. Ruiz, C. Li, S. Ketten, B. A. Helms, T. Xu, *J. Am. Chem. Soc.* **2011**, *133*, 15296–15299.
- [8] C. Reiriz, M. Amorin, R. Garcia-Fandiño, L. Castedo, J. R. Granja, *Org. Biomol. Chem.* **2009**, *7*, 4358–4361.
- [9] a) A. Som, S. Matile, *Eur. J. Org. Chem.* **2002**, *2002*, 3874–3883; b) B. Baumeister, N. Sakai, S. Matile, *Angew. Chem. Int. Ed.* **2000**, *39*, 1955–1958; *Angew. Chem.* **2000**, *112*, 2031–2034; c) S. Matile, *Chem. Soc. Rev.* **2001**, *30*, 158–167.
- [10] a) B. P. Benke, N. Madhavan, *Chem. Commun.* **2013**, *49*, 7340–7342; b) B. P. Benke, N. Madhavan, *Bioorg. Med. Chem.* **2015**, *23*, 1413–1420.
- [11] See the Supporting Information for details.

- [12] The structure was solved in the space group C2 with *R* factor of 4.09%. The unit cell parameters are: a 26.576(4), b 9.7095(11), c 18.779(4). *Z* = 2, *Z'* = 0, *V* = 4503.67 Å³. CCDC-1008786 (1a) contains the supplementary crystallographic data for this paper. These data can be obtained free of charge from The Cambridge Crystallographic Data Centre via www.ccdc.cam.ac.uk/data_request/cif.
- [13] a) K. Kano, J. H. Fendler, *Biochim. Biophys. Acta Biomembr.* **1978**, 509, 289–299; b) N. R. Clement, J. M. Gould, *Biochemistry* **1981**, 20, 1534–1538; c) N. Madhavan, E. C. Robert, M. S. Gin, *Angew. Chem. Int. Ed.* **2005**, 44, 7584–7587; *Angew. Chem.* **2005**, 117, 7756–7759.
- [14] B. A. McNally, A. V. Koulov, B. D. Smith, J.-B. Joos, A. P. Davis, *Chem. Commun.* **2005**, 1087–1089.
- [15] a) F. G. Riddell, M. K. Hayer, *Biochim. Biophys. Acta Biomembr.* **1985**, 817, 313–317; b) D. Milano, B. Benedetti, M. Boccalon, A. Brugnara, E. Iengo, P. Tecilla, *Chem. Commun.* **2014**, 50, 9157–9160.
- [16] a) S. Bhosale, S. Matile, *Chirality* **2006**, 18, 849–856; b) T. Saha, S. Dasari, D. Tewari, A. Prathap, K. M. Sureshan, A. K. Bera, A. Mukherjee, P. Talukdar, *J. Am. Chem. Soc.* **2014**, 136, 14128–14135; c) A. Vargas Jentzsch, S. Matile, *J. Am. Chem. Soc.* **2013**, 135, 5302–5303.
- [17] a) C. De Cola, S. Licen, D. Comegna, E. Cafaro, G. Bifulco, I. Izzo, P. Tecilla, F. De Riccardis, *Org. Biomol. Chem.* **2009**, 7, 2851–2854; b) T. M. Fyles, C.-W. Hu, H. Luong, *J. Org. Chem.* **2006**, 71, 8545–8551.
- [18] <http://www.avantilipids.com/>.

Received: March 5, 2015

Published online on June 3, 2015